Nitrogen doped-ZnO/n-GaN heterojunctions

Xin Yi Chen,[1] Fang Fang,[1] Alan M. C. Ng,[1] Aleksandra B. Djurišič,[1,a)] Kok Wai Cheah,[2] Chi Chung Ling,[1] Wai Kin Chan,[3] Patrick W. K. Fong,[4] Hsian Fei Lui,[4] and Charles Surya[4]
[1]*Department of Physics, The University of Hong Kong, Pokfulam Road, Hong Kong*
[2]*Department of Physics, Hong Kong Baptist University, Kowloon Tong, Hong Kong*
[3]*Department of Chemistry, The University of Hong Kong, Pokfulam Road, Hong Kong*
[4]*Department of Electronic and Information Engineering, Hong Kong Polytechnic University, Hung Hom, Hong Kong*

(Received 30 September 2010; accepted 11 March 2011; published online 21 April 2011)

Nitrogen-doped ZnO nanorods were prepared by electrodeposition using two different Zn precursors (zinc nitrate and zinc acetate), while all other growth conditions (dopant precursor, concentration, growth temperature, and bias) were identical. We have shown that the precursor used affects the properties of the ZnO nanorods, and that the presence of rectifying properties in n-GaN/N:ZnO heterojunctions is strongly related to the use of nitrate precursor for ZnO growth. The difference in the properties of ZnO obtained from two precursors is attributed to the differences in native defect and impurity concentrations, which could affect the electronic properties of the samples. © *2011 American Institute of Physics*. [doi:10.1063/1.3575178]

I. INTRODUCTION

ZnO is a material of considerable interest for optoelectronic applications due to its wide bandgap and high exciton binding energy,[1,2] as well as a variety of nanostructured morphologies and deposition methods.[2] However, one of the factors which is hindering further development of ZnO-based optoelectronic devices is a difficulty in *p*-type doping.[1,3,4] Among different possible acceptor dopants for ZnO, nitrogen has been regarded as one of the most suitable acceptors due to its similar atomic size and electronic structure to oxygen,[3] and hence, it has been extensively studied.[5–16] However, *p*-type conductivity in N:ZnO remains controversial.[3,4] Recent theoretical calculations indicated that nitrogen is a deep acceptor,[5] although hole binding energy derived from PL experiments on N:ZnO was comparable to that observed for Mg in GaN,[4] indicating that nitrogen is a shallow acceptor.[4] Also, the binding energy of the nitrogen acceptor as low as 81 meV has been reported for N:ZnO nanowires.[9] Nitrogen typically substitutes oxygen as N_O acceptor,[4,6] but it can be compensated by various donor defects,[3,4] such as hydrogen for example,[11] and consequently controversial reports on conductivity type of N:ZnO may arise.

In addition to other compensating donors present in undoped ZnO, nitrogen molecules at an oxygen site $(N_2)_O$ are also donors,[3,4,7,8] so that the choice of nitrogen source has a significant influence on the doping. *P*-type conductivity in N:ZnO, grown by variety of methods and with different nitrogen sources, has been reported to date.[9–16] In addition, in spite of the concerns on the reproducibility and stability of *p*-type doping in ZnO,[1,4] stable *p*-type conductivity for five months of storage in air was reported for N:ZnO.[9] Consequently, nitrogen doping for the achievement of *p*-type ZnO has significant potential, provided that native and other compensating defects can be controlled to avoid compensation. In this work, we have used a simple, low-cost and low-temperature solution-based growth method, namely electrodeposition,[17,18] to prepare N:ZnO and ZnO nanorods. Ammonium nitrate was used as the source of nitrogen since it has been successfully used for nitrogen doping of ZnO nanoparticles by a different synthesis method.[19,20] In addition to the advantages in terms of low-growth temperature and simplicity, we expect that the compensation effects due to $(N_2)_O$ would be smaller than in the case of vapor phase deposition.

II. EXPERIMENTAL DETAILS

The nanorod arrays were fabricated on indium tin oxide (ITO) glass substrates and GaN films on sapphire (cleaned by sonication in toluene, acetone, ethanol, and de-ionized water). ITO substrates were used for determination whether the top contact on ZnO nanorods is ohmic or rectifying. GaN films have been grown on sapphire substrates by metal organic chemical vapor deposition (MOCVD) using a Thomas swan MOCVD system. The *n*-GaN sample structures were sapphire/30 nm GaN buffer layer/2.2 μm *n*-GaN (Si:GaN, $n = 5 \times 10^{17}$ cm^{-3})/1.1 μm *n*-GaN (Si:GaN, $n = 3 \times 10^{18}$ cm^{-3}) or sapphire/30 nm GaN buffer layer/2.2 μm undoped GaN/2.2 μm *n*-GaN ($n = 5 \times 10^{17}$ cm^{-3}). The GaN substrate used had a small effect on the optical properties of ZnO (small change in the ratio of UV to defect emission) and the resistance of the LEDs/slope of the I-V curve under forward bias, but overall behavior trends for different precursors and introduction of *N* dopant was the same for both GaN substrates. Electrodeposition was performed using a two electrode setup (Pt foil as anode, substrate as cathode) at a constant temperature of 80°C and bias of 10 mA for 1 min and 1 mA for 29 min. The electrolyte consisted of aqueous solution (deionized water, 60 ml) of Zn precursor (zinc nitrate hydrate, Aldrich, 99.999% purity, 8 mM or zinc acetate, Aldrich, 99.999% purity, 8 mM) and

a)Electronic mail: dalek@hku.hk.

hexamethylenetetramine (Aldrich, 99+ % purity, 8 mM). For *N* doped samples, ammonium nitrate (Aldrich, 99.5% purity, 0.8 mM) was added.

The morphology of the samples was examined by scanning electron microscopy (SEM) using a JEOL JSM-7001F SEM, while photoluminescence (PL) spectra were measured using a HeCd laser (325 nm) as an excitation source and the emission spectra were collected using a monochromator (Acton SpectraPro 500i) with Peltier-cooled photomultiplier detector (Hamamatsu R636-10). The composition of the samples was characterized by time of flight secondary ion mass spectroscopy (TOF SIMS V) using ION-TOF GmbH and Auger Electron Spectroscopy (AES) using PHI 5600 (Physical Electronics; electron energy 5 keV, area 1 μm diameter circle). Transmission electron microscopy (TEM), high resolution transmission electron microscopy (HRTEM) and selected area electron diffraction (SAED) were performed using Philips Tecnai G2 20 S-TWIN. Electron energy loss spectroscopy (EELS) was performed using JEOL 2010F TEM and Philips Tecnai F20 TEM equipped with EELS.

For GaN/ZnO heterojunction devices, Al(100 nm)/Ag(200 nm) contacts were deposited onto *n*-GaN and the contacts were verified to be ohmic. Then, after the ZnO nanorod growth the space between the nanorods has been filled using spin-on-glass (SOG, Futurex, Inc.) or poly(-methyl methacrylate) (PMMA) to prevent short circuit between the top electrode and the n-GaN layer. SOG was spin-coated at 3000 rpm for 40 s, followed by annealing at 200°C for 1 min. For this spin-coating condition, the space between the nanowires was filled with SOG while the tops of the nanowires were covered with negligible amount of SOG (verified by SEM and ohmic contact check in the structure ITO/ZnO + SOG/Ag or Au). For PMMA layer, solution of 2% PMMA in chlorobenzene was spin-coated at 4000 rpm for 45 s, followed by baking at 200 °C for 1 min. Then, oxygen plasma was used to etch the PMMA to expose the tops of the nanorods. Then, the top electrode (Ag, 200 nm or Au, 60 nm) was evaporated in through a shadow mask (1 mm radius) using a thermal evaporator AST PEVA 500 EL. I-V curves were measured using a Keithley 2400 source meter.

III. RESULTS AND DISCUSSION

Figure 1 shows the SEM images of ZnO nanorods electrodeposited on *n*-GaN substrate using nitrate and acetate precursors, with and without doping (samples DN = nitrate precursor, doped; UN = nitrate precursor, undoped; DA = acetate precursor, doped; UA = acetate precursor, undoped). It can be observed that nitrate precursor results in more densely packed nanorods with improved orientation with respect to the substrate compared to acetate precursor. The addition of the dopant for both precursors improves the density of the packing. In the case of UA samples, it can be observed that the nanorod growth is sparse, with some uncovered areas of the substrate.

To study the quality of the nanorods, variable temperature PL measurements have been performed and the obtained

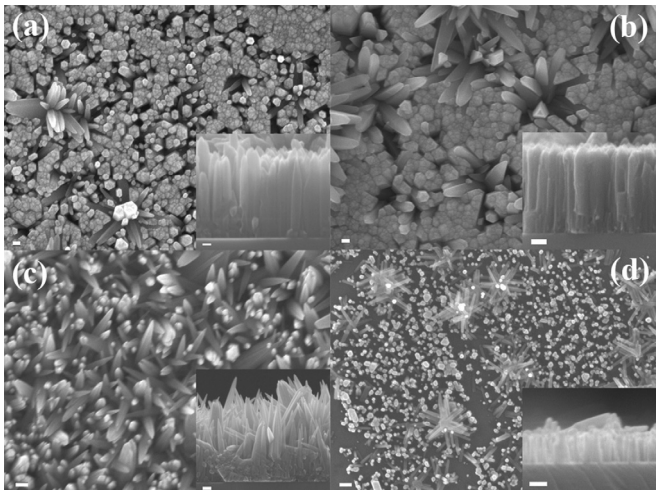

FIG. 1. SEM images of (a) *N* doped and (b) undoped ZnO nanorods using nitrate precursor; (c) *N* doped and (d) undoped ZnO nanorods using acetate precursor. The scale bars are 100 nm.

results are shown in Figs. 2 and 3. It can be observed that at low temperatures all the samples exhibit prominent UV emission. For UA sample, two emission peaks are observed in the UV region, with the shorter wavelength peak likely originating from the *n*-GaN substrate. At room temperature, defect emission in the orange-red spectral region is observed. This kind of defect emission is commonly observed in solution grown samples, and it was attributed to defect complexes and associated with the presence of surface adsorbates, such as OH groups, on the surface.[21] Visible emission was most prominent in the UA sample, but this could originate from the n-GaN film (also shown in the inset of Fig. 2(d) for comparison). Since this sample has the lowest nanorod density and the UV emission from *n*-GaN can also be observed in addition to UV emission from ZnO, the visible emission likely contains contributions from *n*-GaN and ZnO. The fact that the emission appears structured, same as in the case of *n*-GaN substrate, is an additional indication that significant part of it originates from *n*-GaN. No visible emission is observed for DA sample, while in the case of nitrate precursor there is some defect emission for both DN and UN samples. It was previously reported that lower defect emission was obtained for the acetate precursor than for nitrate precursor for hydrothermally grown ZnO films on p-GaN (Ref. 22). While we indeed obtain lower defect emission for DA samples, in the case of UA samples contribution of the substrate is likely the cause of the different behavior compared to previous work, in addition to the different growth method and conditions (precursor concentration, growth temperature, etc.) used in this work.

At 15 K, we can observe significant difference between different samples. Both samples with acetate precursor show blue-shifted emission compared to nitrate precursor, with peak position at 3.372 eV for DA and 3.377 eV for UA, which are possibly due to ionized donor bound exciton for DA[23,24] and free exciton for UA.[24] A possible candidate for the ionized donor resulting in peak position at 3.372 eV is gallium impurity, which would be an expected impurity for

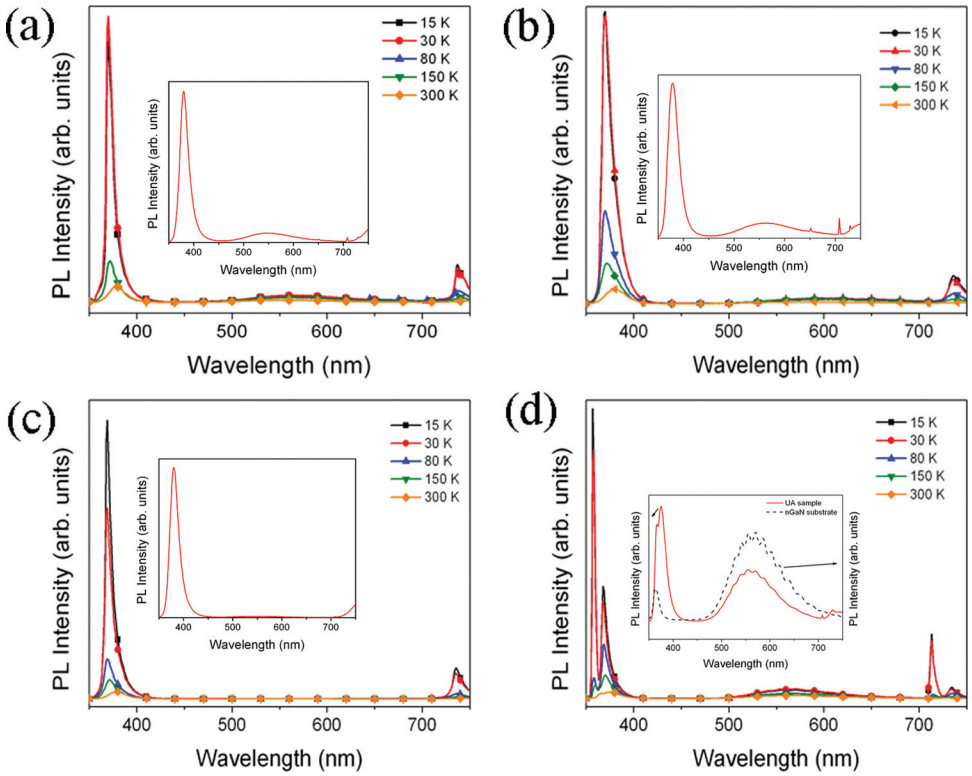

FIG. 2. (Color online) Variable temperature PL spectra of (a) *N* doped and (b) undoped ZnO nanorods using nitrate precursor; (c) *N* doped and (d) undoped ZnO nanorods using acetate precursor.

the growth on GaN.[23] UN sample exhibits a single broad peak at 3.372 eV, but this peak is more broad than in the case of DA sample which could be due to superposition of two or more peaks. DN sample exhibits the most complex spectrum out of all the samples studied. The emission peak is narrower compared to UN sample, indicating a possible improvement in the sample quality in agreement with the reduction of defect emission. In this case as well the dominant peak is at 3.367 eV, and a shoulder at ~3.377 eV likely corresponding to free exciton emission[24] can also be resolved. In addition to these, there is also a prominent feature at ~3.33-3.34 eV which is absent in all the other samples. This emission can be attributed to acceptor-bound excitons and it was previously observed in nominally undoped p-type ZnO (Ref. 25). Thus, it likely originates from acceptors or acceptor complexes which can be present without the introduction of the dopant. Also, the emission lines in this spectral region are typically attributed to native defects.[12] The peaks related to nitrogen doping at ~3.31-3.315 eV (acceptor bound exciton),[12,14] and 3.24 eV donor-acceptor pair (DAP) emission[14] could not be clearly resolved, although from the shape of the peak contributions in this spectral region cannot be excluded.

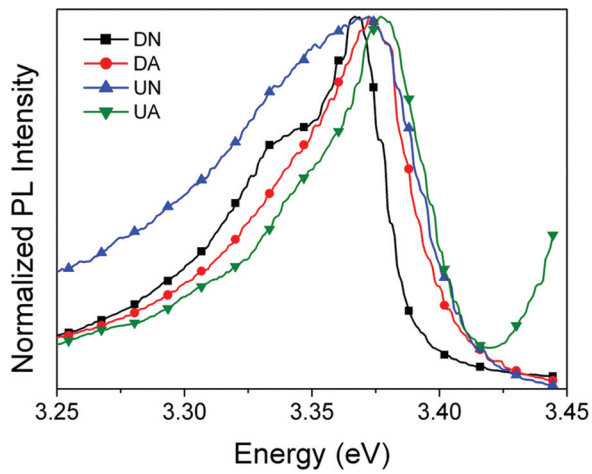

FIG. 3. (Color online) Normalized PL spectra of samples prepared using different precursors at 15 K.

The I-V curves of the samples are shown in Fig. 4. It can be observed that in the case of SOG larger leakage current is observed compared to a polymer insulating layer similar to our previous work,[26] but in all cases DN samples exhibited clear rectifying properties. Rectification ratio at 3V was 16.5 for DN sample with PMMA, and 14.9 for DN sample with SOG. In contrast, the corresponding values for DA sample were only 5.7 and 1.4, respectively. For undoped samples, it can be observed that the nitrate precursor results in presence of some rectification, while this is not the case for acetate precursor. Also, while both Ag and Au result in ohmic contacts to ZnO nanorods grown on ITO, this is not the case for ZnO nanorods grown on nGaN, indicating that the substrate used affects the nanorod properties. If one of the contacts resulted in an ohmic I-V characteristics, we would consider that sample to not exhibit rectifying behavior. Thus, robust rectifying behavior was only observed in DN samples (for both Ag and Au contacts), while for UN sample with Ag contact nonlinear but almost symmetric I-V curve is observed. It should be noted that *p*-type conduction[26] and ambipolar charge transport[27] were observed

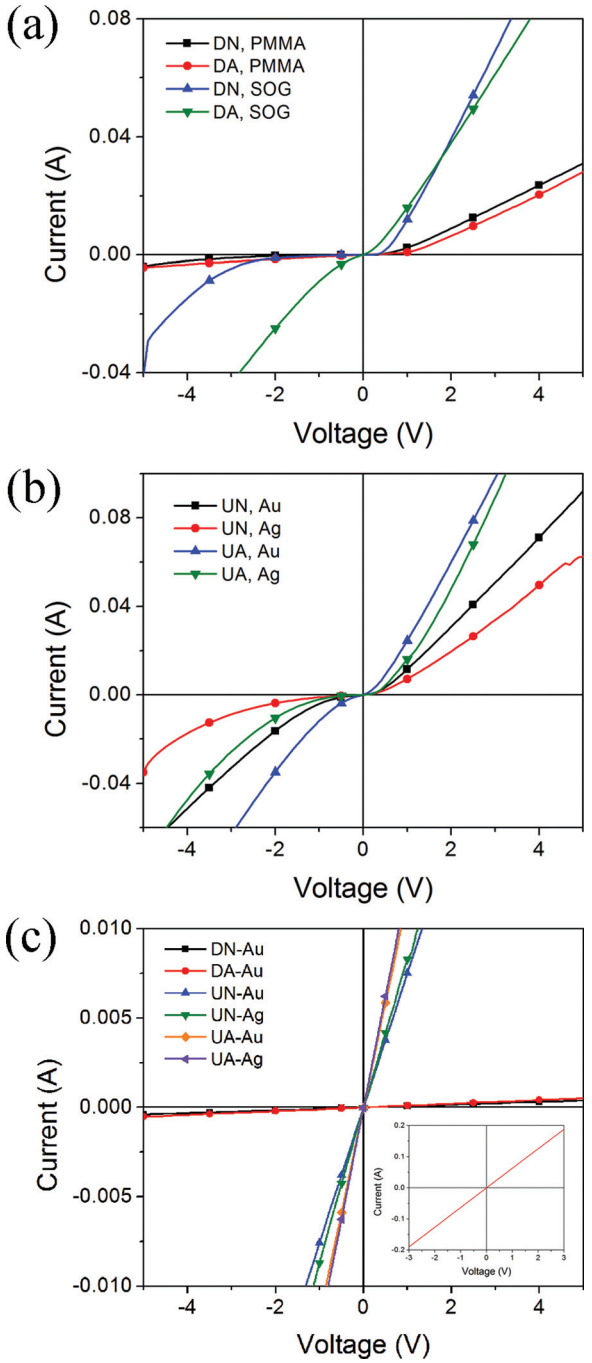

FIG. 4. (Color online) I-V curves of (a) doped samples with different dielectric between the rods (b) undoped samples with different metal electrode (c) ohmic contact check for the structure ITO/ZnO nanorods + SOG/Au or Ag. The inset shows ohmic contact check for Al/Ag contact on GaN.

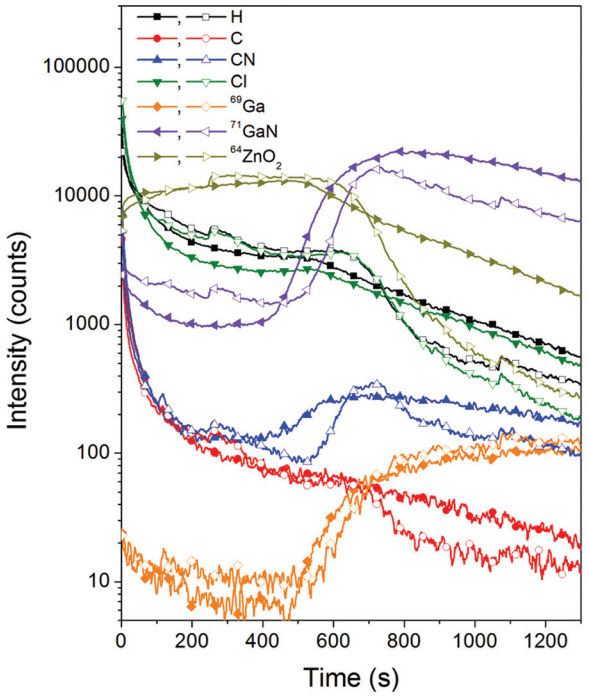

FIG. 5. (Color online) SIMS profiles for DN (closed symbols) and DA (open symbols) samples.

previously in hydrothermally grown ZnO nanorods from nitrate[26] and chloride[27] precursors. In case of nitrate precursor, observed behavior was attributed to an increased concentration of zinc vacancies and decreased concentration of donor impurities.[26]

To further investigate the causes of observed behavior, we studied the composition of the samples using AES and TOF-SIMS. SIMS was used in order to obtain hydrogen profiles in the samples since hydrogen is expected to be a common donor impurity.[3] Also, it was proposed that hydrogen can compensate nitrogen doping in ZnO.[11] The obtained SIMS profiles for DN and DA samples are shown in Fig. 5. Direct comparison of the curves is somewhat difficult due to difference in density and orientation of the nanorods (more dense and better oriented nanorods for DN sample), but it can be clearly observed that there is a higher hydrogen and chlorine concentration in the DA sample. Chlorine is also a donor in ZnO (Ref. 28), and it can be incorporated during electrochemical growth from solution containing Cl ions.[28] Chlorine ions also tend to preferentially adsorb onto (0001) ZnO surface,[29] and thus they may get incorporated into the nanowires during growth at a low concentration. Chlorine impurities in our samples were unexpected since no chlorine was deliberately introduced. However, hexamethylenetetramine can contain anionic impurities, which are mainly Cl^- and SO_3^-.

There are also some differences in the nitrogen-containing ion profiles, but they are not very conclusive. Therefore, AES measurements were performed to obtain better information on the nitrogen content in the samples. For each sample, several spots were tested due to some variations in the nanorod packing and orientation across the substrate. AES results confirmed presence of Cl in all the samples. No nitrogen signal was observed in UN and DA sample. Cl content in DA sample varied from 1.5% to 2.0%. In UA samples, nitrogen signal is observed together with the signal from Ga, which is likely due to the sparse nanorod growth so that signals from substrate can be observed. In DN samples, chlorine content was from 0.8% to 1.6%. As for nitrogen, in some probing positions no significant nitrogen peak was found, while in others clear nitrogen signal is observed, as shown in Fig. 6. The highest nitrogen content observed was 5.5%. The

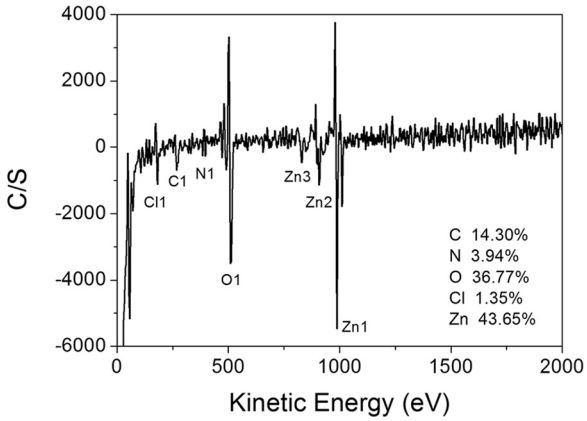

FIG. 6. AES spectrum of DN sample.

variation in the composition from one spot to another is likely due to relatively small beam size (1 μm diameter) and the fact that some parts of the sample contain nanorods which are not well oriented [see Fig. 1(a)].

The sample composition and structure has been further examined using TEM and EELS, and the obtained representative results are shown in Fig. 7. It can be observed that DN samples exhibit good crystallinity, while for DA samples some cases obvious defect areas can be observed in HRTEM images. TEM results are consistent with the low temperature PL spectra, where more clearly resolved and narrower features in DN samples indicate possibly better crystal quality compared to DA samples. In terms of sample composition, similar to AES, some variation can be observed between different nanorods. However, nitrogen signal in the EELS spectra can be more commonly found in DN samples compared to DA samples. The majority of the DA samples exhibits no signal in the range 400-450 eV, while for DN samples majority of samples exhibit signal in that range. The nitrogen spectrum in all cases is relatively noisy, but this was also the case for the reference spectrum obtained from BN sample (shown in the inset of Fig. 7).

Thus, the precursor used has a significant effect on the nitrogen incorporation. For example, for ZnO nanoparticles it has been shown that the incorporation of nitrogen was dependent on nitrogen precursor, but opposite trends were obtained for two different precursors used for ZnO.[19,20] However, the properties of the samples are likely a complex interplay of native defects and donor and acceptor impurities. Which type of defects are going to dominate is strongly dependent on the deposition conditions. Nevertheless, we have reproducibly obtained rectifying behavior in N:ZnO/n-GaN heterojunctions (although no light emission under forward bias up to 20 V was observed), while no such behavior was observed for acetate precursor.

To study further the diode performance of N:ZnO/n-GaN heterojunctions, we have performed fitting of the measured data, as shown in Fig. 8(a). The I-V curve of a *p-n* junction diode can typically be described by an equation, $I = I_s[\exp(qV/nkT) - 1]$, where n is the ideality factor and I_s is the reverse saturation current.[15,30,31] The obtained ideality factor for the region 0.01-0.4 V is $n = 3.1$. This is

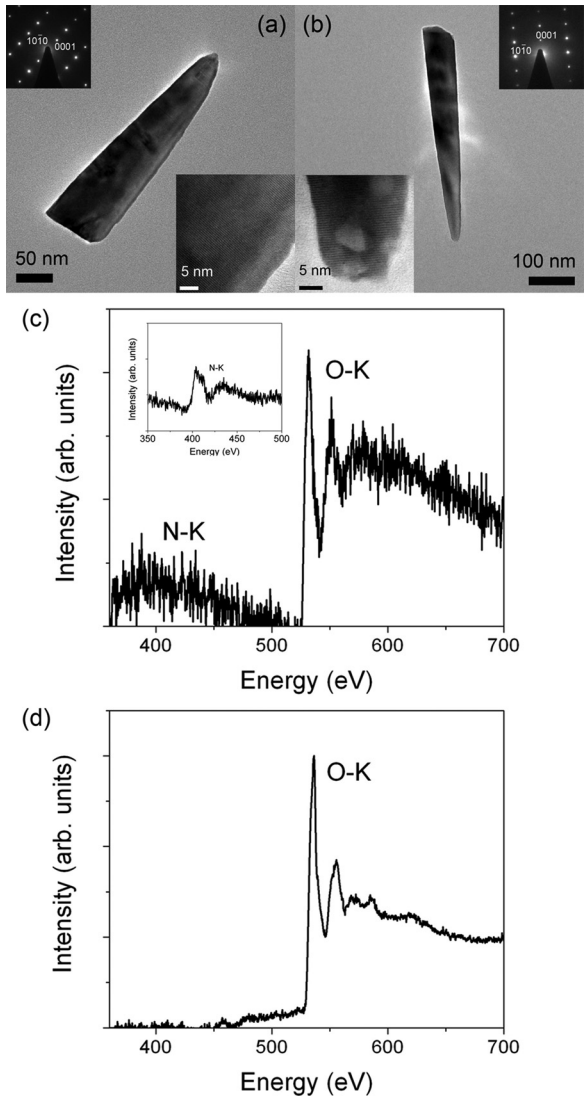

FIG. 7. (a)–(b) TEM of DN and DA samples; The insets show the corresponding HRTEM images and SAED patterns (c)–(d) EELS spectra of DN and DA samples. The inset shows reference nitrogen spectrum from BN sample.

lower than that previously reported for p-ZnO/n-Si heterojunction (~4),[13] and significantly lower than that previously reported a ZnO homojunction diode (~24).[16] In general, ideality factors of wide bandgap semiconductor heterojunctions are usually high, although in some reports ideality factors below two have been achieved.[32] Ideality factors higher than two can occur if the actual junction can be modeled as a series of diodes, as well as if tunneling across the junction occurs.[30] Tunneling can also result in a linear $I \sim V$ dependence at low voltages,[32] but in our case linear region occurs only at very low voltages (<0.04 V). At higher bias voltages, dependence $I \sim V^2$ attributed to the space charge limited current is typically observed.[13,15,32] However, fitting the I-V curve in the region 0.4-5 V with exponential function $I = a V^m$ resulted in $m = 1.44$. This is close to a value of $m = 1.5$ which has been previously observed in different heterojunctions,[31,33,34] and which can occur in the case of double injection of carriers,[31] injection from a point contact,[33] and

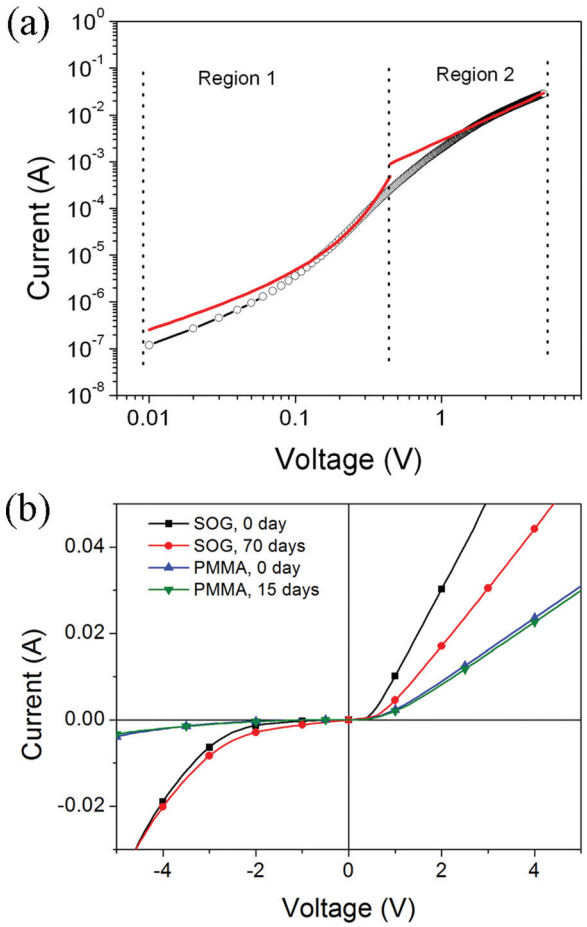

FIG. 8. (Color online) (a) Experimental and fitted I-V curve of DN sample with PMMA (b) Comparison of I-V curves of DN samples immediately as prepared and after storage in low vacuum.

presence of a trap density gradient.[34] From the SIMS profiles, impurity gradients in the samples are obvious, and since the samples are nanorods, than the geometry factors (point contact) may also contribute to the observed value of *m*. Overall, the observed behavior of N:ZnO/n-GaN heterojunction is similar to other wide bandgap material *p-n* junctions reported in the literature.

Finally, a significant concern with *p*-type doping of ZnO is its stability. Previous reports on N:ZnO nanowires indicated that the *p*-type doping was stable for over five months of ambient storage, although carrier concentration gradually decreased, likely due to adsorption of oxygen molecules onto nanowire surfaces.[9] Therefore, we have stored the samples in low vacuum. The I-V curves measured after storage are shown in Fig. 8(b). It can be observed that the electronic properties of the N:ZnO samples remain stable under such storage conditions.

IV. CONCLUSIONS

We have prepared ZnO nanorods (with and without nitrogen doping) using two different precursors. We found that the precursor used affected the nanorod morphology, density and orientation, as well as its optical properties, native defects and impurity incorporation. Stable and reproducible rectifying properties were observed for N:ZnO (nitrate precursor)/n-GaN heterojunctions. The observed behavior can be attributed to the complex interplay between native defects and impurity incorporation (higher acceptor and lower donor impurities).

ACKNOWLEDGMENTS

Financial support from the Strategic Research Theme, University Development Fund, Small Project Grant, and Innovation & Technology Fund (Grant No. ITS/129/08) is acknowledged. The authors would like to thank MCPF, Hong Kong University of Science and Technology for SIMS and AES measurements. The authors would like to thank Department of Physics, Chinese University of Hong Kong and Materials Preparation and Characterization Facility, the Hong Kong University of Science and Technology for EELS measurements.

[1]A. B. Djurišić and Y. H. Leung, Small **2**, 944 (2006).
[2]Ü. Özgür, Ya. I. Alivov, C. Liu, A. Teke, M. A. Reshchikov, S. Doğan, V. Avrutin, S. -J. Cho, and H. J. Morkoç, J. Appl. Phys. **98**, 041301 (2005).
[3]A. Janotti and C. G. Van de Walle, Rep. Prog. Phys. **72**, 126501 (2009).
[4]M. D. McCluskey and S. J. Jokela, J. Appl. Phys. **106**, 071101 (2009).
[5]J. L. Lyons, A. Janotti, and C. G. Van de Walle, Appl. Phys. Lett. **95**, 252105 (2009).
[6]D. C. Look, Semicond. Sci. Technol. **20**, S55 (2005).
[7]Y. F. Yan, S. B. Zhang, and S. T. Panelides, Phys. Rev. Lett. **86**, 5723 (2001).
[8]L. Li, C. X. Shan, B. H. Li, B. Yao, J. Y. Zhang, D. X. Zhao, Z. Z. Zhang, D. Z. Shen, X. W. Fan, and Y. M. Lu, J. Phys. D: Appl. Phys. **41**, 245402 (2008).
[9]G. D. Yuan, W. J. Zhang, J. S. Jie, X. Fan, J. A. Zapien, Y. H. Leung, L. B. Luo, P. F. Wang, C. S. Lee, and S. T. Lee, Nano Lett. **8**, 2591 (2008).
[10]T. Zaidi, A. Melton, W. E. Fenwick, and I. Ferguson, J. Vac. Sci. Technol. B. **27**, 1904 (2009).
[11]J.-L. Zhao, X.-M. Li, J.-M. Bian, W.-D. Yu, and C.-Y. Zhang, J. Cryst. Growth. **280**, 495 (2008).
[12]W. Mu, L. Guo, L. L. Kerr, and D. C. Look, Mater. Res. Soc. Symp. Proc. **1201**, 1201-H02-08 (2010).
[13]S. Majumdar and P. Banerji, J. Appl. Phys. **105**, 043704 (2009).
[14]I. V. Rogozin and M. B. Kotlyarevsky, Semicond. Sci. Technol. **23**, 085008 (2008).
[15]M. Dutta and D. Basak, Appl. Phys. Lett. **92**, 212112 (2008).
[16]Y. G. Cao, L. Miao, S. Tanemura, M. Tanemura, Y. Kuno, and Y. Hayashi, Appl. Phys. Lett. **88**, 251116 (2006).
[17]M. Willander, O. Nur, Q. X. Zhao, L. L. Yang, M. Lorenz, B. Q. Cao, J. Zúñiga Pérez, C. Czekalla, G. Zimmermann, M. Grundmann, A. Bakin, A. Behrends, M. Al-Suleiman, A. El-Shaer, A. Che Mofor, B. Postels, A. Waag, N. Boukos, A. Travlos, H. S. Kwack, J. Guinard and D. L. Dang, Nanotechnology **20**, 332001 (2009).
[18]X.-J. Wu, F. Zhu, C. Mu, Y. Q. Liang, L. F. Xu, Q. W. Chen, R. Z. Chen and D. S. Xu, Coord. Chem. Rev. **254**, 1135 (2010).
[19]N. Uekawa, Y. Mitani, T. Kojima and K. Kakegawa, J. Ceram. Soc. Jpn. **117**, 283 (2009).
[20]N. Uekawa, T. Kojima and K. Kakegawa, J. Mater. Res. **24**, 3343 (2009).
[21]A. B. Djurišić, Y. H. Leung, K. H. Tam, Y. F. Hsu, L. Ding, W. K. Ge, Y. C. Zhong, K. W. Wong, W. K. Chan, H. L. Tam, K. W. Cheah, W. M. Kwok, and D. L. Phillips, Nanotechnology **18**, 095702 (2007).
[22]T. Sahoo, J.-W. Ju, V. Kannan, J. S. Kim, Y.-T. Yu, M.-S. Han, Y.-S. Park, and I.-H. Lee, Mater. Res. Bull. **43**, 502 (2008).
[23]B. K. Meyer, J. Sann, S. Lautenschläger, M. R. Wagner and A. Hoffmann, Phys. Rev. B **76**, 184120 (2007).
[24]B. K. Meyer, H. Alves, D. M. Hofmann, W. Kriegsels, D. Forster, F. Bertram, J. Christen, A. Hoffmann, M. Straβburg, M. Dworzak, U. Haboeck, and A. V. Rodina, Phys. Status Solidi B **241**, 231 (2004).
[25]Y. J. Zeng, Z. Z. Ye, W. Z. Xu, J. G. Lu, P. H. He, L. P. Zhu, B. H. Zhao, Y. Che, and S. B. Zhang, Appl. Phys. Lett. **88**, 262103 (2006).

[26]Y. F. Hsu, Y. Y. Xi, K. H. Tam, A. B. Djurišić, J. M. Luo, C. C. Ling, C. K. Cheung, A. M. C. Ng, W. K. Chan, X. Deng, C. D. Beling, S. Fung, K. W. Cheah, P. W. K. Fong, and C. C. Surya, Adv. Funct. Mater. **18**, 1020 (2008).
[27]C.-Y. Wong, L.-M. Lai, S.-L. Leung, V. A. L. Roy, and E. Y.-B. Pun, Appl. Phys. Lett. **93**, 023502 (2008).
[28]J. Rousset, E. Saucedo, and D. Lincot, Chem. Mater. **21**, 534 (2009).
[29]R. Tena-Zaera, J. Elias, G. Wang, and C. Lévy-Clément, J. Phys. Chem. C. **111**, 16706 (2007).
[30]J. H. He and C. H. Ho, Appl. Phys. Lett. **91**, 233105 (2007).
[31]J. A. Edmond, K. Das, and R. F. Davis, J. Appl. Phys. **63**, 922 (1998).
[32]N. Koteeswara Reddy, Q. Ahsanulhaq, and B. H. Hahn, Appl. Phys. Lett. **93**, 083124 (2008).
[33]M. A. Lampert, A. Many, and P. Mark, Phys. Rev. **135**, A1444 (1964).
[34]Y. Watanabe, Phys. Rev. B **81**, 195210 (2010).